The 2010 IEEE/RSJ International Conference on
Intelligent Robots and Systems
October 18-22, 2010, Taipei, Taiwan

Power Assist Method for a Nonholonomic Mobile Robot using both ZMP Criterion and Impedance Control

Hiroshi Hidaka, Yoshiro Hada, Yuichi Murase and Shinji Kanda,
FUJITSU LABOLATORIES LTD.

***Abstract*—In this paper, we describe a power assist method for a nonholonomic mobile robot designed to carry out office-oriented services. We developed a new mechanism for obtaining an approximate measurement of the zero moment point (ZMP) using three single-axis force sensors so that a robot pushed from any direction by a human can detect the direction and magnitude of the external force. We also propose impedance control to generate translational and rotational motion in accordance with ZMP displacement. This control method achieves a function whereby a robot that has been given an external force from a direction differing from its translation direction will follow the direction of the external force while rotating. The robot can also return automatically to its initial pose once the external force has been released. We show though experiments that our power assist method is effective in improving the operability and usability of an office-oriented robot.**

I. INTRODUCTION

Recently, expectations for service robots that can coexist with humans have been increasing. In response to these expectations, we have developed a mobile service robot for use in office environments. A photograph of this robot is shown in **Fig. 1,** and its specifications are listed in **Table 1**. Robot applications include transport services for documents, magazines, beverages, snacks, and so on and information services provided via a touch panel display on the robot's table top. The robot has a circular shape to facilitate communication with surrounding workers. A nonholonomic mobile mechanism using two driving wheels is adopted as the vehicle unit of the robot.

We have verified through trials that the robot can move about autonomously within an office and execute transport tasks. In a cramped office environment, however, we found that the robot bumped into people and impede passage when stopped. In response to this problem, it is necessary to easily move the robot out of the way by pushing it from any direction.

In research related to such physical interaction between humans and robots, various power assist method have been proposed. Maeda et al. developed a power-assisted cart that could be easily moved about despite its 700-kg weight by applying an external force to a handgrip equipped with three gap sensors [1], and Kitagawa et al. developed a power assist system for use in wheelchairs [2]. In these types of equipment, however, the operable component is restricted to a specific part of the robot such as a handgrip.

For the sake of enhanced operability, it would be better if the external-force detection component on the robot's exterior covered a wide area allowing the robot to be pushed from any place other than a handgrip. Furthermore, considering that most office staff know nothing about how the robot moves and operates, it is necessary for the robot to move according to a person's intention when pushed from any direction. In addition, if an excessive external force is applied to the robot, a means for detecting danger of falling down is needed.

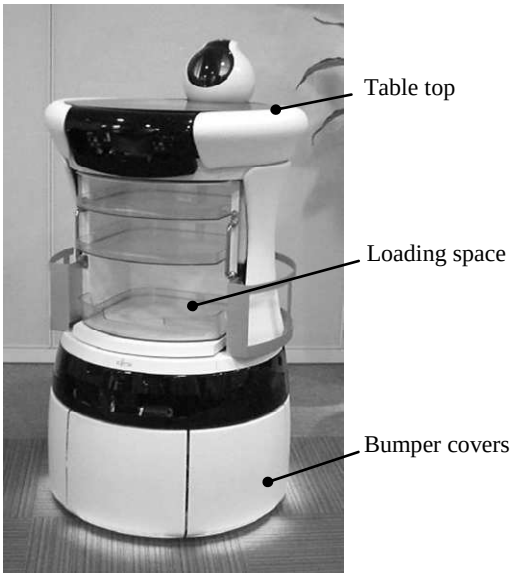

Fig. 1 Photograph of robot

Table 1 Specifications of office robot

Item	Value
Exterior size	ϕ0.6[m] by 1.2[m] tall
Weight	65[kg]
Maximum velocity	1.2[m/s]
Maximum ascent ability	1/12(5[degree])
Maximum loading weight	20[kg]
Number of driving wheels	2

FUJITSU LABORATORIES LTD. 10-1 Morinosato-Wakamiya, Atsugi 243-0197, Japan (tel: +81-46-250-8218; fax: +81-46-250-8841; e-mail: hidaka @jp.fujitsu.com, hada.yoshiro@jp.fujitsu.com, murase.yuuichi@jp.fujitsu. com, s.kanda@jp.fujitsu.com)

We have also examined a recovery method to be applied after a person moves the robot. The robot moves in an office environment autonomously using path planning based on a map and estimating its pose with integrated information from stereo vision cameras and distance sensors. However, the robot cannot return to the target trajectory if it loses its pose when pushed or moved to an unknown place. Even if its pose can be identified, there is a possibility that the robot will encounter unknown obstacles on a new route toward the target trajectory. In our research, we have determined that the robot should recover the position and orientation just before application of the external force for the robot to perform stably and robustly.

Based on the above discussion, the required functions for this robot can be summarized as follows:

(1) Detect external force from any direction around the robot

(2) Assess stability, i.e., risk of falling down

(3) Move in direction of push and automatically return to original pose after external force is released

To implement functions (1) and (2), we focused on the zero moment point (ZMP), which is generally used as a criterion for evaluating stability in bipedal robots [3]-[5]. If an external force is applied to a robot, the ZMP undergoes a displacement enabling the direction and magnitude of the external force to be determined. Additionally, if the ZMP approaches the boundary enclosed by the robot's wheels' ground contact points, the risk of falling can be detected. Although the ZMP can be generally determined from the reaction force applied to a ground contact point, it is difficult for a wheel-based mobile robot to detect a reaction in a wheel's ground contact point. Komoriya et al. proposed a control method using the ZMP criterion to stabilize a pose of a mobile manipulator with driving wheels [6]. Although their method can detect the risk of the falling down, a mechanism to detect the ZMP is rather complex. With this in mind, we developed a simple mechanism for estimating the ZMP using three single-axis force sensors and derived the direction and magnitude of the external force from the displacement of the estimated the ZMP. In addition, we implemented programs to judge whether an external force is a person's operating force or not. For example, the programs detect package loads by measuring the normal force and update the default position of the ZMP, and correct the ZMP displacement on a slope by using values of acceleration sensors.

To implement function (3), we focused on the impedance control methods used in human-robot cooperative tasks [7]-[10]. However, these impedance control methods target stable movement as intended by a human and does not take into account robot recovery. We therefore focused our attention on the elasticity term of the impedance control law and devised a method for having the robot automatically and stably return to its state immediately before the external force was applied despite a nonholonomic mechanism.

We developed a power assist method for a nonholonomic mobile robot with two driving wheels using the ZMP for detecting any directional forces and impedance control. The paper is organized as follows. Section II describes a new mechanism for measuring the ZMP in our newly developed wheel-based mobile robot and a method for approximating the ZMP. Section III describes the power assist method. based on the ZMP. Section IV presents the results of a verification experiment using an actual robot with the proposed method. Section V concludes the paper.

II. ZMP Estimation Method

A. Measurement model for estimating ZMP displacement

In this section, we describe the sensor arrangement in a wheel-based mobile robot and a method for estimating the ZMP.

Fig. 2 illustrates the application of an external force $\boldsymbol{F}$ in a horizontal direction at a certain height h. The robot body with a total mass m consists of upper and lower units: an upper body with mass m_2 and a lower vehicle unit with mass m_1 made up of heavy components such as a battery and power-supply controller. Three single-axis force sensors (VALCOM VPW6KC3) are installed between these two units and arranged at equal intervals of 120 degrees around the periphery of the robot at a height near the ground.

This sensor arrangement can improve detection sensitivity of external forces since the vehicle unit's heavy load, which does not fluctuate, is not measured. Denoting the ZMP as $\boldsymbol{p} = [p_x, p_y]^{\mathrm{T}}$, as observed from the robot's coordinate system when applying external force $\boldsymbol{F} = [F_x, F_y]^{\mathrm{T}}$ to the robot in the horizontal direction, p_x and p_y can be given by the following expressions:

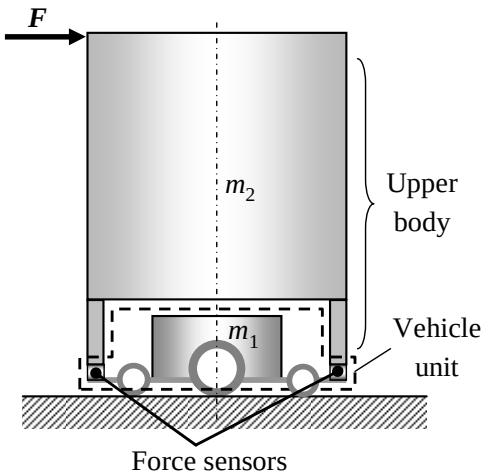

Fig. 2 Robot Configuration

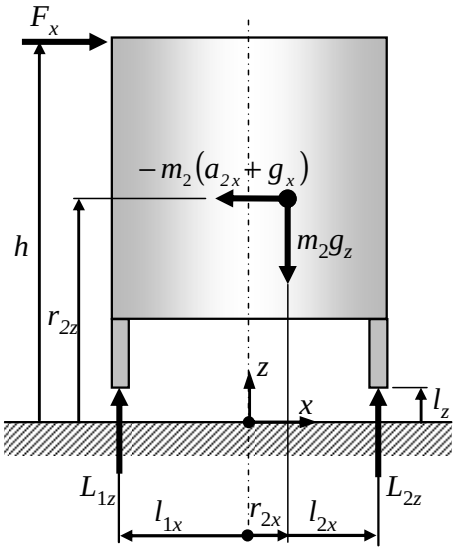

Fig. 3 Mechanical model of upper body

$$p_x = \frac{\sum_i m_i(a_{iz}+g_z)r_{ix} - \sum_i m_i(a_{ix}+g_x)r_{iz} + F_x h}{\sum_i m_i(a_{iz}+g_z)} \quad (1)$$

$$p_y = \frac{\sum_i m_i(a_{iz}+g_z)r_{iy} - \sum_i M_i(a_{iy}+g_y)r_{iz} + F_y h}{\sum_i m_i(a_{iz}+g_z)} \quad (2)$$

(i = 1, 2)

where $[m_i a_{ix},\ m_i a_{iy},\ m_i a_{iz}]^{\mathrm{T}}$ is inertia force, $[r_{ix},\ r_{iy},\ r_{iz}]^{\mathrm{T}}$ is the center-of-gravity vector of the ith mass, and $\boldsymbol{g} = [g_x, g_y, g_z]^{\mathrm{T}}$ is the gravity-acceleration vector.

It can be seen from Eqs. (1) and (2) that the ZMP also varies according to h. Therefore, it cannot be determined whether ZMP displacement is caused by the magnitude of the external force or h of the external force. We assume that in most cases the external force is applied to the robot at the height around the robot's tabletop because the shape of the robot is designed like a drum and people are led to put their hands on the table top. In fact, we found that most people pushed the tabletop, and if their hands were full, they tried to push the upper part of the robot using their elbows or waists. If the lower part of the robot is pushed, the robot stops because the lower surfaces consist of bumper covers detecting contact as shown in **Fig. 1**.

Fig. 3 shows a mechanical model of the robot's upper body on the xz-plane. All of the external force sensors are installed at the same height, and the position vector of a force sensor with respect to the robot's coordinate system is denoted as $\boldsymbol{l}_j = [l_{jx},\ l_{jy},\ l_z]^{\mathrm{T}}$ (j = 1 to 3). Given that the force sensors are arranged near the ground contact surface so that l_z is sufficiently smaller than h and r_{2z}, the balance of moments in the upper body can be given by the following equations:

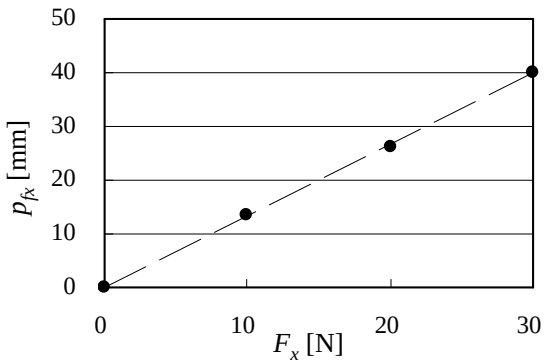

Fig. 4 Relation between ZMP and external force

$$m_2 g_z r_{2x} - m_2(a_{2x}+g_x)r_{2z} + F_x h = \sum_j L_j l_{jx} \quad (3)$$

$$m_2 g_z r_{2y} - m_2(a_{2y}+g_y)r_{2z} + F_y h = \sum_j L_j l_{jy} \quad (4)$$

We assume that the operating environment for the office robot conforms to the barrier-free law in Japan. This law dictates that the maximum gradient of an inclined surface is 1/12 (about 5 degrees). Since change in g_z due to this maximum incline is less than 1%, we can treat g_z as being constant regardless of the incline so that $g_z \approx g$ and $a_{iz} \approx 0$. The ZMP can therefore be given by the following expressions from these approximations and Eqs. (1) - (4).

$$p_x = \frac{m_1 g r_{1x} - m_1 a'_x r_{1z} + \sum_j L_j l_{jx}}{mg} \quad (5)$$

$$p_y = \frac{m_1 g r_{1y} - m_1 a'_y r_{1z} + \sum_j L_j l_{jy}}{mg} \quad (6)$$

where $[a'_x, a'_y]^{\mathrm{T}} = [a_{ix}+g_x, a_{iy}+g_y]^{\mathrm{T}}$ is measured from a 2-axis acceleration sensor.

Based on the above discussion, we can compute an estimated ZMP using Eqs. (5) and (6).

B. Verification of estimated ZMP

Using the office robot shown in **Fig. 1**, we conducted two experiments to check the validity of the estimated ZMP derived in the previous section.

First, we examined the relationship between external force $\boldsymbol{F}$ and ZMP displacement. Assuming that the robot is in a stationary state, we measured ZMP displacement $\boldsymbol{p}_f = [p_{fx}, p_{fy}]^{\mathrm{T}}$ when an external force $\boldsymbol{F} = [F_x, F_y]^{\mathrm{T}}$ is applied at a fixed height h. The relationship between F_x and p_{fx} is shown in **Fig. 4**. External force F_x was applied at 10 N increments up to 30 N. The error between the approximating line and p_{fx} was within ±1%. These results indicate that F_x and p_{fx} have a nearly linear relationship. Similar results were obtained along the y-axis, so if we denote the ZMP displacement vector as $\boldsymbol{p}_f$

= $[p_{fx},\ p_{fy}]^T$, the following relationship holds between $\boldsymbol{p}_f$ and external force $\boldsymbol{F}$:

$$\boldsymbol{p}_f = K_f \boldsymbol{F} \tag{7}$$

Next, we examined the validity of this estimated ZMP. As an object of comparison, we used $\boldsymbol{p}_W$, the ZMP calculated from the reactive forces at the wheels' ground contact points. The contact-ground reactive forces were measured by keeping the robot stationary and arranging single-axis force sensors between the wheels and the ground. Denoting the position vector of the wheels' ground contact points as $\boldsymbol{w}_i$ and the vertical component of the reactive force at $\boldsymbol{w}_i$ as W_{iz}, $\boldsymbol{p}_W$ can be given by the following expression:

$$\boldsymbol{p}_W = \frac{\sum_i \boldsymbol{w}_i W_{iz}}{mg} \tag{8}$$

Now, denoting the $\boldsymbol{p}_W$ displacement vector due to $\boldsymbol{F}$ as $\boldsymbol{p}_{Wf}$, **Fig. 5** compares $\boldsymbol{p}_f$ and $\boldsymbol{p}_{Wf}$ when applying $\|\boldsymbol{F}\|$ = 20 N from four equidistant directions along the robot's periphery. Examining these results, we see that $\boldsymbol{p}_{Wf}$ exhibits equivalent displacements in the directions of these external forces. If we therefore consider external forces applied from all directions, the resulting displacement would lie along the dashed circle in this figure. The direction of $\boldsymbol{p}_f$ is nearly the same as true value $\boldsymbol{p}_{Wf}$, and we can therefore conclude that the results for the estimated ZMP are valid.

III. Power Assist Method

In this section, we describe a power assist method. With this method, the office robot can follow the direction of an external force applied from a direction other than its translation motion by using rotational motion (**Fig. 6**(a)) and it can return to its initial pose after the external force is released (**Fig. 6**(b)).

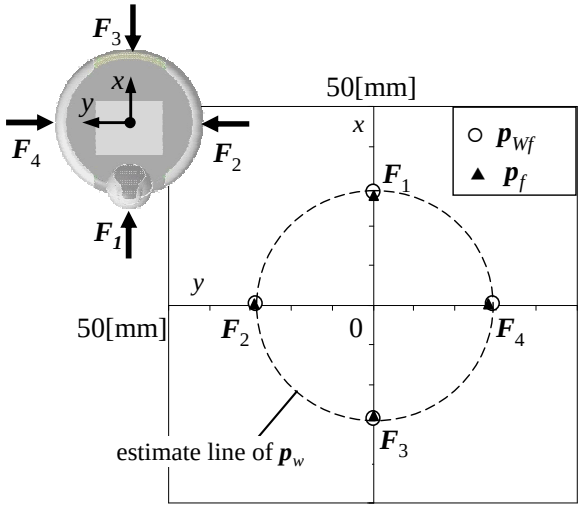

Fig. 5 Comparison of true value $\boldsymbol{p}_{Wf}$ and measured value $\boldsymbol{p}_f$

A. Virtual model to follow direction of external force

Fig. 7(a) depicts the pushing of the robot with $\boldsymbol{F}$ by a human with the robot in its initial pose. This robot, however, cannot move in the *y* direction due to a nonholonomic constraint. So it is necessary for the robot to rotate itself when subjected to an external force applied from a direction other than the *x* direction so that its wheels face the direction of that external force. We therefore propose the virtual model shown in **Fig. 7**(b) in which any point (*d*, 0) on the x-axis is pulled by $\boldsymbol{F}$. This model results in the application of accelerating torque $F_y d$ to the robot and the generation of angular velocity. Here, *d* can be given as follows, where $d_0 > 0$:

$$d = \begin{cases} d_0 & ; F_x \geq 0 \\ -d_0 & ; F_x < 0 \end{cases} \tag{9}$$

We set d_0 = 0.3 m under the assumption that the edge of the tabletop is pulled.

B. Impedance model for power assist

In this section, we describe a robot drive method when an external force is applied. **Fig. 8** shows robot pose $\boldsymbol{X} = [x, y, \theta]^T$ after being pulled by a virtual force. The robot estimates $\boldsymbol{X}$ by odometry and knows its pose even though the amount and direction of an external force continuously change. When the robot recovers the pose just before the external force was applied, it estimates its pose using stereo vision cameras and distance sensors and starts to move along a target trajectory. In this figure, the spatial coordinate system is denoted as O-*xy* and the robot's coordinate system is denoted as O'-*x*'*y*'. The robot's pose immediately before the external force was applied is given as $\boldsymbol{X} = [0, 0, 0]^T$. Here, $\boldsymbol{F}$ in the spatial coordinate system can be replaced by $\boldsymbol{F}' = [F'_{x'}, F'_{y'}]^T$ in the robot's coordinate system. Movement in the translational and rotational directions can be given by the following impedance model:

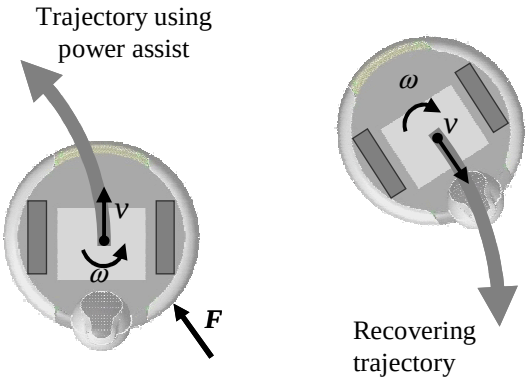

(a) external force is applied (b) external force is released

Fig. 6 Robot's motion using combination of translation and rotation

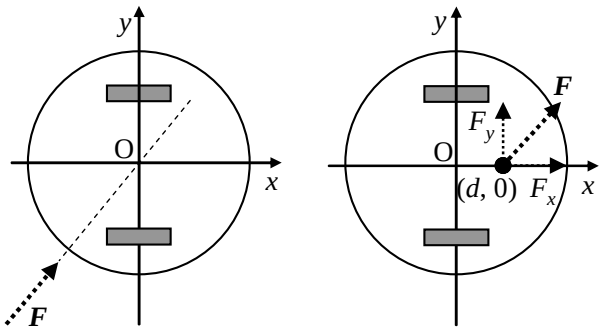

(a) Practical model (b) Virtual model

Fig. 7 Models of applying external force

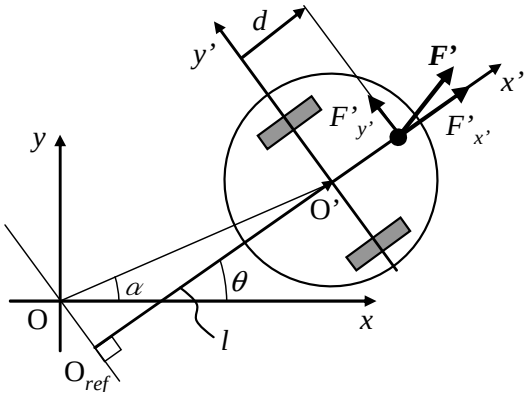

Fig. 8 Dynamics of applying operating force

$$M\dot{v} + Bv + Kl = F'_{x'} \tag{10}$$

$$I\dot{\omega} + B_\theta \omega = F'_{y'}\, d \ , \tag{11}$$

where M is inertia, B is viscous modulus, K is elastic modulus, I is moment of inertia, B_θ is rotating viscous modulus, v is translational velocity, ω is angular velocity, and l is distance $O_{ref}O'$ given by the following equation:

$$l = (x\cos\alpha + y\sin\alpha)\cos(\theta - \alpha)\ , \tag{12}$$

where $\alpha = \tan^{-1}(y / x)$.

From Eqs. (10) and (11), the robot can follow the direction of an externally applied force through movement having impedance characteristics.

C. Impedance model for recovery

We present a method for returning the robot to its initial pose $[0, 0, 0]^T$ from any pose $\boldsymbol{X} = [x, y, \theta]^T$ when the external force is released. An external force $\boldsymbol{F'}$ is defined as $[0, 0]^T$ in Eqs.(10) and (11), the robot returns to position O_{ref}, as shown in **Fig. 8,** since there is no elasticity term in the rotational direction. To correct this, we propose a method for returning the robot to origin O while its orientation changes by giving Eq. (11) an elasticity term.

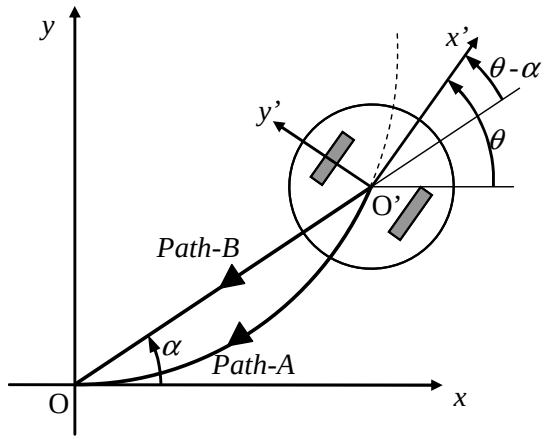

Fig. 9 Recovery path back to origin

Table 2 Parameters of impedance control model

	Item	Value
d_0	Torque Arm Length	0.3 [m]
M	Inertia	30 [kg]
I	Moment of Inertia	1.35 [kg·m^2]
B	Viscous Modulus	90 [N/(m/s)]
B_θ	Rotating Viscous Modulus	4.05 [Nm/(rad/s)]
K	Elastic Modulus	30 [N/m]
K_θ	Torsional Elastic Modulus	3 [Nm/rad]

Canudas et al. introduced a trajectory-generation method using a circle tangent to the x-axis and passing through the origin and the robot's axis of rotation, as shown by *Path-A* in **Fig. 9** [11]. With this method, however, the recovery path might turn into a long detour depending on the orientation of the robot. Considering that the trajectory of a robot that has just been pushed transitions from rotational motion to translational motion, it would be desirable if the trajectory at the time of recovery would transition from translational motion to rotational motion. Thus, the trajectory at the time of recovery can be given by *Path-B*. The equation of motion along this trajectory is given by the following equation:

$$M\dot{v} + Bv + Kl = 0 \tag{13}$$

$$I\dot{\omega} + B_\theta \omega + K_\theta(\theta - \alpha) = 0 \tag{14}$$

Then, when robot position (x, y) reaches the origin, the robot rotates and returns to its original orientation so that $\alpha = 0$. While returning to the origin, high stability is required. We have established the following overdamping conditions so that the robot's approach has no oscillating movements:

$$B > 2\sqrt{MK} \tag{15}$$

$$B_\theta > 2\sqrt{IK_\theta} \tag{16}$$

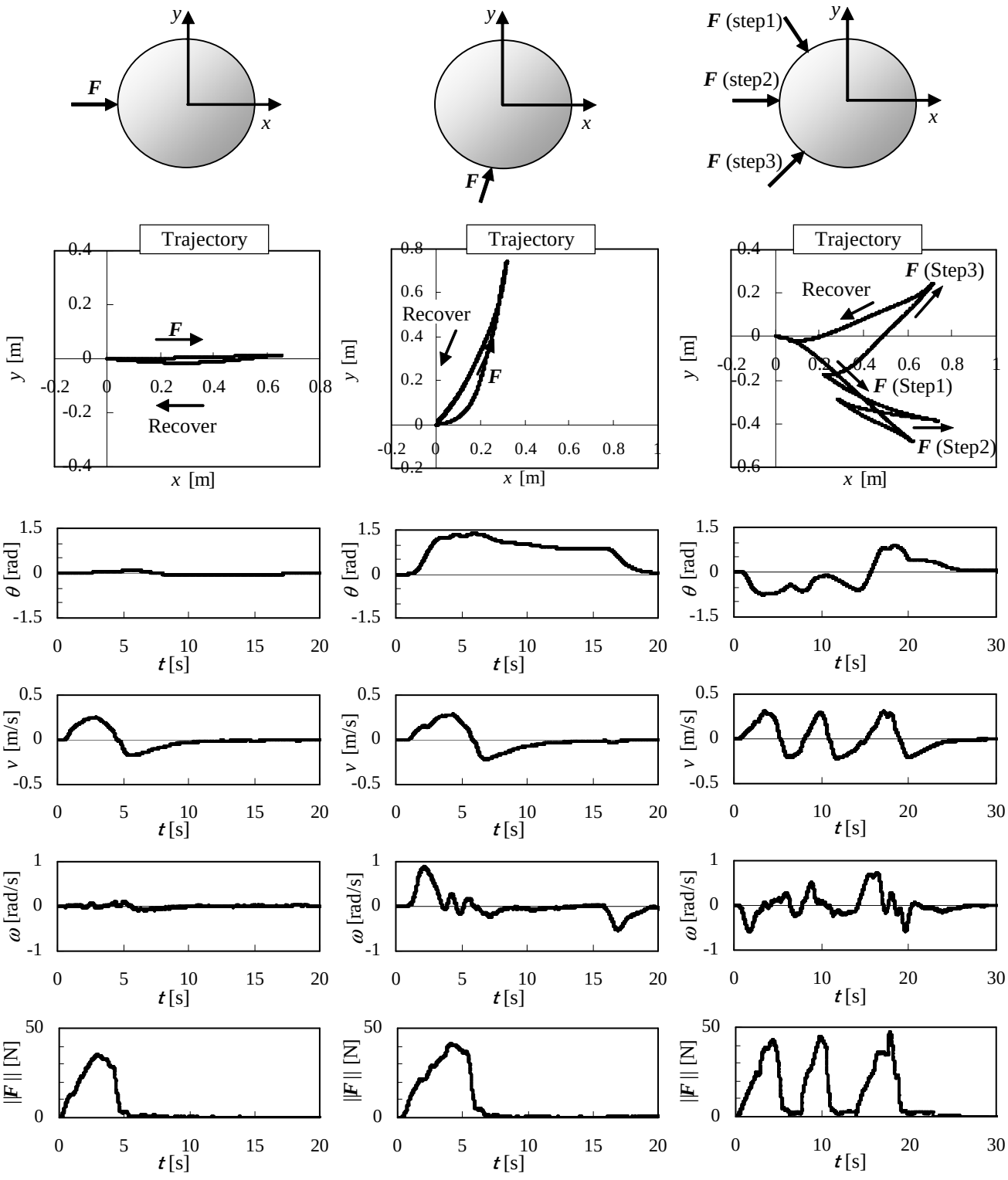

(a) 0 degrees between $\boldsymbol{F}$ and x-axis

(b) 80 degrees between $\boldsymbol{F}$ and x-axis

(c) Intergraded angle between $\boldsymbol{F}$ and x-axis

Fig.10 Examples of robot's resultant trajectories, $\|\boldsymbol{F}\|$, θ, v, and ω for various applied forces

IV. EXPERIMENT

To examine the effectiveness of the impedance control law presented in section III, we experimentally tested robot's movement using our power assist method.

A. Experimental Condition

Impedance-control parameters used in experiments are listed in **Table 2**. These parameters were set from the following perspective. We assume that if an external force equivalent to what people generally use to push open a door could be used to move a robot out of the way, people would not feel it strange to apply such a force to a robot. We therefore measured the force applied on opening a door using several subjects and found that the peak force was about 30 N and that the time required to open the door was about 2 s.

We then set inertia M and viscous modulus B so that the target speed would be 0.3 m/s when the robot is pushed in the translational direction by a force of 30 N and so that at least 90% of the target speed would be reached after 1 s. Next, for rotational direction, we set $I = Mr^2/2$ under the assumption that the shape of the robot is cylindrical with a radius $r = 0.3$ m, and on the basis of these values, we set viscous modulus B_θ so that at least 90% of this target speed would be reached after 1 s. We assumed that a force of 30 N would move the robot 1 m (which we took to be a sufficient distance for people to pass), and to satisfy condition (15), we set K. We gave the torsional elastic modulus K_θ its maximum value to satisfy condition (16).

B. Results of Experiment

Fig. 10 shows the resulting trajectories and changes in orientation, velocity, angular velocity, and external force over time when the robot is pushed in various directions. The results in **Fig. 10**(a) show that the robot moved in nearly a straight line when pushed in the translational direction. The results in **Fig. 10**(b), moreover, show that the robot, when pushed in a direction other than the translation direction, proceeded to move in a translation direction while performing a rotational operation to move in the direction of the externally applied force.

Furthermore, from **Fig. 10**(c), we can see that the robot moved in the direction of the external force even when the direction of that force changed in a stepwise manner. Thus a human can move the robot out of the way to the desired direction even if the mobility is nonholonomic constant.

The trajectory graphs also show that the robot returned to its initial position in a stable manner along a linear trajectory. On returning to that position, θ converged to 0 and we confirmed that the robot could return to its initial pose stably.

By envisioning real-world conditions that may occur, we conducted an experiment to see how the robot would go about a recovery when situated behind a door in a stationary state and pushed when an person opens the door (**Fig. 11**). In **Fig. 11**(a), the door starts to open, and in **Fig. 11**(b), an external force is applied to the robot via the door, causing the robot to move away. Finally, in **Fig. 11**(c)-(d), the door is once again shut and the robot has returned to its initial pose. Thus, we confirmed the high degree of usability.

V. CONCLUSION

We dealt with the problem of a robot interrupting people's passage in office environments. To solve this problem, we proposed a power assist method based on the ZMP and impedance control for a nonholonomic mobile robot using two driving wheels. The results of this research are summarized below:

1) We developed a simple mechanism for estimating ZMP by appropriately arranging several single-axis sensors. Using this estimated ZMP, we derived the direction and magnitude of an external force applied to the robot. Additionally, safety was improved by applying the ZMP to a function for detecting the risk of falling.
2) We confirmed that applying impedance control to the behavior of a nonholonomic mobile robot caused the robot to move in the direction of an applied external force and to return to its original pose after the external force was released. As a result, office staffs who knew nothing about the configuration of the robot could move the robot out of the way with simple manual operation, resulting in improved operability and usability of the robot.

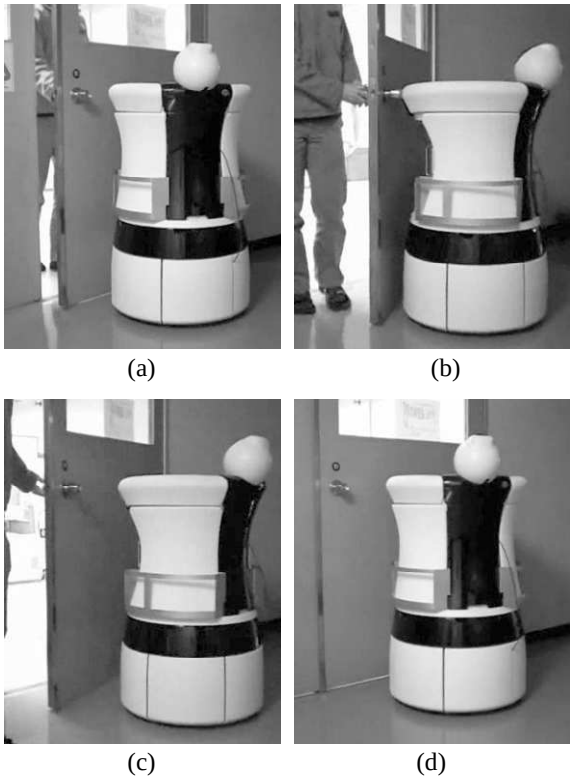

Fig. 11 Behavior of robot when pushed with door

Although the method we proposed was shown to be effective using an office robot, it represents technology that can be applied to all kinds of service robots designed to coexist with humans. We expect this technology to have a wide range of applications in the future.

VI. ACKNOWLEDGMENTS

This research was conducted using a robot developed under the New Energy and Industrial Technology Development Organization (NEDO) “Project for Strategic Development of Advanced Robotics Elemental Technologies” and supported by Okamura Corporation and Fujitsu Design Limited.

REFERENCES

[1] H. Maeda, S. Fujiwara, H. Kitano, H. Yamashita, "Control of an Omni-directional Power-assisted Cart" JSME international journal. Series C, Mechanical systems, machine elements and manufacturing, vol.46, No.3, 2003.

[2] H. Kitagawa, K. Terashima, T. Miyoshi, J. Urbano, S. Nishisaka, "Power Assist System for Omni-directional 'zkansport Wheelchair Using Fuzzy Reasoning" Proc. IEEE Int. Conf. Control Applications, vol. 1, pp. 123-130, 2004.

[3] M. Vukobratovi´c and J. Stepanenko: ”On the Stability of Anthropomorphic Systems,” Mathematical Biosciences, vol.15 pp.1-37, 1972

[4] Q. Li, A. Takanishi, I. Kato, "A Biped Walking Robot Having A ZMP Measurement System Using Universal Force-Moment Sensors," Proc. IEEE/RSJ Int. Conf. Intelligent Robots and Systems, vol. 3, pp. 1568-1573, 1991.

[5] K. Erbatur, A. Okazaki, K. Obiya, T. Takahashi, A. Kawamura, "A study on the zero moment point measurement for biped walking robots," 7th International Workshop Advanced Motion Control, pp. 431-436, 2002.

[6] K. Komoriya, K. Yokoi and T. Koyoku: “Motion Control of Omni-directional Mobile Manipulation for Indoor Environment,” Proceedings of IEEE International Workshop on Robot and Human Interactive Communication, pp. 274-279, 2001.

[7] M. Sato, K. Kosuge, "Handling of Object by Mobile Manipulator in Cooperation with Human using Object Trajectory Following Method," Proc. IEEE/RSJ Int. Conf. Intelligent Robots and Systems, vol. 1, pp. 541-546, 2000.

[8] K. Kosuge, M. Sato, N. Kazamura, "Mobile robot helper" Proc. IEEE Int. Conf. Robotics and Automation, vol. 1, pp. 583 - 588, 2000.

[9] H. Arai, T. Takubo, Y. Hayashibara, K. Tanie, "Human-Robot Cooperative Manipulation Using a Virtual Nonholonomic Constraint," Proc. IEEE lnt. Conf. Robotics and Automation, Vol. 4, pp. 4063-4069, 2000.

[10] T. Takubo, H. Arai, K. Tanie, "Human-Robot Cooperative Handling Using Virtual Nonholonomic Constraint in 3-D space," Proc. IEEE Int. Conf. Robotics and Automation, vol. 3, pp. 2680-2685, 2001.

[11] C. Canudas de Wit, 0. J. Sordalen, "Exponential Stabilization of Mobile Robots with Nonholonomic Constraints," IEEE Trans. Automatic Control, vol. 37, no. 11, pp. 1791-1797, 1992.